ASTM INTERNATIONAL
Standards Worldwide

Geotechnical
Testing Journal

Ali Tolooiyan,[1] Rae Mackay,[2] and Jianfeng Xue[3]

DOI: 10.1520/GTJ20140028

Measurement of the Tensile Strength of Organic Soft Rock

VOL. 37 / NO. 6 / NOVEMBER 2014

Geotechnical Testing Journal

doi:10.1520/GTJ20140028 / Vol. 37 / No. 6 / November 2014 / available online at www.astm.org

Ali Tolooiyan,[1] Rae Mackay,[2] and Jianfeng Xue[3]

Measurement of the Tensile Strength of Organic Soft Rock

Reference

Tolooiyan, Ali, Mackay, Rae, and Xue, Jianfeng, "Measurement of the Tensile Strength of Organic Soft Rock," *Geotechnical Testing Journal*, Vol. 37, No. 6, 2014, pp. 1–11, doi:10.1520/GTJ20140028. ISSN 0149-6115

ABSTRACT

Understanding all potential slope failure mechanisms is a pre-requisite for predicting the likelihood of batter movements during excavation in open cut mines. The tensile behavior of soils and rocks may be a significant contributor to a slope failure and must be known in order to quantify the risks of slope failure. The contribution can be particularly significant for Intermediate Geotechnical Materials (IGMs) that possess characteristics of both soils and rocks and where the failure mechanisms are complex due to the interplay between ductile and brittle behavior. Brown coal is such an intermediate geotechnical material. Recent batter movements in the brown coal mines in the Latrobe Valley, Australia have raised doubts about the current understanding of the mechanisms of slope failure in this material. Research is underway to re-evaluate all properties of the brown coal applicable to slope failure. This paper describes the investigation of brown coal tensile strength. There are alternative test methods available to determine the tensile behavior of materials, including direct tensile tests, beam bending tests and Brazilian compression tests. The applicability of each test method is material dependent and, as such, it is necessary to confirm the validity of the methods for each material. Beam bending tests have achieved mixed results for both rocks and IGMs previously. Thus, the present work has explored only the use of Direct tensile and Brazilian test methods. Both methods were implemented using a modified direct shear apparatus and valid test procedures for both test methods were developed. Each test procedure has been verified by Finite Element Modelling (FEM) using ABAQUS 6.12.1 FEM code. The results from the laboratory test methods are in good agreement and show that brown coal is a predominantly brittle material with a peak tensile strength slightly greater than 100 kPa. The finite element analyses confirm that non-uniformity of the tensile stresses during sample loading tends to lead to the underestimation of tensile strength for both tests, but the Brazilian test has less bias for brown coal. It is observed that the rate of

Manuscript received February 10, 2014; accepted for publication August 6, 2014; published online September 19, 2014.

[1] Geotechnical and Hydrogeological Engineering Research Group (GHERG), Federation University Australia, Building 4W, Northways Road, Churchill, VIC 3842, Australia,
e-mail: tolooiyan@gmail.com

[2] Professor, Geotechnical and Hydrogeological Engineering Research Group (GHERG), Federation University Australia, Building 4W, Northways Road, Churchill, VIC 3842, Australia,
e-mail: rae.mackay@federation.edu.au

[3] School of Engineering and IT, Federation University Australia, Building 4W, Northways Road, Churchill, VIC 3842, Australia,
e-mail: jianfeng.xue@federation.edu.au

loading of low stiffness, low permeability, and saturated samples in the Brazilian test is an important test design parameter for the accurate determination of tensile strength of IGMs in the laboratory.

Keywords

tensile strength, intermediate geotechnical material, laboratory testing, geotechnical modeling, brown coal

Introduction and Background

Intermediate Geotechnical Materials (IGMs) span geo-materials from brittle soils to soft rocks. Many engineering applications including open cut mining require a good understanding of the geo-mechanical behavior of these materials. One property of interest is the tensile strength of IGMs. Although early researchers (e.g., Hudson 1969) suggested that tensile strength of weak rocks should not be considered as a material physical property, tensile strength may impact different failure modes for problems such as slope stability, ground drilling, and open-cut and underground mining when part of the in situ compressive stress is released due to excavation. Tensile strength must also be determined to measure other mechanical properties of soft rocks, such as horizontal stress and undrained shear strength, from in situ field measurements, such as pressuremeter testing (Haberfield 1997).

During the last forty years, significant attention has been paid to methods of measuring rock tensile strength including the examination of the influence of rock anisotropy (Exadaktylos and Kaklis 2001; Cai and Kaiser 2004; Coviello et al. 2005; Yu et al. 2006; Li and Wong 2013).

Potentially, the best method for measuring tensile strength of solid materials is a pure direct tensile test (DTT). For this test, a sample, usually cylindrical, is axially loaded to failure by tensile forces applied at the ends of the sample. For brittle materials, it is assumed that sample cross section area is constant and stress is uniformly distributed over the failure cross section. In this case, the tensile strength (S_t) is measured as the ratio between the applied force (F) at failure and the cross section area (A): $S_t = F/A$.

Unfortunately, these assumptions are rarely valid and the measured tensile strength is not necessarily accurate. The axial stress may be non-uniform over the sample cross section due to sample shape and the heterogeneity of the material, leading to underestimation of tensile strength (Coviello et al. 2005). Moreover, practical application of a tensile stress test requires a mechanism for gripping the sample at either end. Stress concentrations may occur at the contact between the sample and the grips and this commonly results in failure mechanisms other than tensile failure. Preparation of rock specimen for a DTT is usually time consuming and expensive; hence this test is not usually performed in rock mechanic laboratories (Butenuth et al. 1995; Coviello et al. 2005; Mellor and Hawkes 1971). Nevertheless, DTT methods have been used by geotechnical researchers to investigate the tensile strength of unsaturated soils, over-consolidated clays, and cemented sands, even though sample preparation is not easy for these materials and test equipment has to be tailored to accommodate the specific soil properties (Ajaz and Parry 1974; Lu et al. 2007; Vesga and Vallejo 2006).

Owing to the difficulties associated with using DTT methods for rocks, several indirect test methods have been developed. These include the beam bending test (BBT) and the Brazilian test (BT). For these methods, tensile failure of a specimen is induced by applying bending moments and compressive forces, respectively. These reduce the sensitivity of the results to the loading method compared with the DTT.

The BBT is popular in civil engineering, especially for measuring the tensile strength of concrete mixtures. For this test, the specimen bar (of either circular or rectangular cross section) is subjected to three or four point bending loads. The tensile strength is then calculated using the well-known Navier's equation. The validity of this test for rock material has been debated in the published literature. Jaeger and Hoskins (1966) and Jaeger (1967) employed DTT and BBT to measure the tensile strength of different rocks with tensile strengths ranging from 3 to 12 MPa. They showed that the BBT gives tensile strengths 150 to 200 % higher than the DDT. Coviello et al. (2005) compared DTT, BBT, and BT on two different soft rocks with tensile strength of 0.4 and 0.65 MPa and suggested that the BBT does not appear to be an appropriate method for determining the tensile strength of weak rocks. In spite of the apparent difficulties, BBT has been successfully used to study the tensile strength and fracture toughness of unsaturated cohesive soils for the purpose of crack propagation in soils (Amarasiri et al. 2011).

The BT is one of the most popular tests for measuring the tensile strength of rocks. In this test, a rock cylinder is diametrically loaded to failure using curved or flat rigid plates. The failure load is then converted to tensile strength using the equation suggested by Mellor and Hawkes (1971). The Mellor and Hawkes equation assumes a linear elastic constitutive behavior for the rock. Since the tensile strength of a rock is much less than its compressive strength and a rock in tension is usually brittle, a tensile fracture should only be initiated where tensile stress develops. This condition is not guaranteed and the validity of indirect tests in which the first fracture initiates in the compressed part of the cylinder has been extensively debated (Colback 1966; Coviello et al. 2005; Hudson et al. 1972).

In 1977, the International Society for Rock Mechanics (ISRM 1977) standardized and proposed the BT as a suggested method for determining the tensile strength of rock material. The BT owes most of its popularity to the ease of specimen preparation, which does not require particular care or expensive shaping techniques (Coviello et al. 2005). Moreover, strength anisotropy in non-isotropic material can be investigated easily (Barla and Innaurato 1973). Owing to the convenience of the BT, this method has been widely employed in different engineering fields in many countries and is considered as the standard method for measuring tensile strength of rock material (e.g., China (GBStandards-T50266-99) and United States of America (ASTM D3967-08)).

The accuracy of the BT has long been debated. Colback (1966) provided a comprehensive discussion of the theory and experimental evidence for the BT. Using Griffith's fracture theory, which takes the friction of compressed cracks into account, he showed that fracture would first initiate at a specimen-loading platen contact point and the extension fracture would then be triggered anywhere in the central third of the specimen. Finally, he concluded that Griffith's criterion ensures that the calculated tensile strength from a BT coincides well the measured value from DTT (Coviello et al. 2005). As the result of other research, Mellor and Hawkes (1971) confirmed that although the DTT cannot be fully substituted by indirect tensile tests, BT provides a good estimation of tensile strength for brittle materials. Yu et al. (2006) and Fahimifar and Malekpour (2012) employed finite element analysis to analyze stress distribution in a BT specimen and confirmed that the BT may marginally underestimate the tensile strength, and a correction factor that takes the dimension of the sample into account should be applied to the test results.

In this paper, DTTs and BTs are carried out on Australian Brown Coal, an over-consolidated organic soft rock, using a modified automatic direct shear test machine. The objective has been to prove the use of the methods and to obtain tensile strength values for the coal for the purpose of slope stability analysis in the large brown coal open cuts in the Latrobe Valley, Victoria. Advanced FEM analysis using models of both tests has been employed for test verification and to analyze the stress concentration across the tension failure plane.

Test Material

Victoria, Australia hosts 23 % of the world's brown coal reserves. It is the largest brown coal deposit in the world (Australia Mineral Resource 2011). More than 80 % of Victoria's 430×10^9 tons of brown coal is located in the Latrobe Valley, 160 km south-east of Melbourne (DPI 2012). Three open-pit mines operate in the valley to supply coal to four coal-fired power stations, which produce most of Victoria's electricity. Australian Brown Coal is a light organic material with a unit weight around 11.5 kN/m^3 and high water content (up to 200 %). Material testing shows that its uniaxial compressive strength can be in the order of 1 MPa and the shear strength is characterized by high cohesion (200 kPa) and friction angle (37°). Coal seams can exceed 100 m in thickness and are separated by interseam materials comprising mixed fluvial bedded silts and gravels and clays. The deepest open cut is now at a depth around 220 m below ground level (Xue and Tolooiyan 2012).

Tectonically controlled sub-vertical joints within the coal seams are frequent and penetrate through the whole depth of the seam. Slope failure may comprise a composite of processes including toppling, sliding, heave, and shear. Sub horizontal joints are observed. The tensile strength of the coal is important for understanding both crack initiation and propagation and the sequence of processes contributing to movement within a coal seam.

Brown coal samples can be readily shaped using basic equipment (routers, drills, saws, and mills). The low stiffness of the coal permits the accurate machining of samples. Laboratory samples of brown coal are also sensitive to environment and undergo rapid moisture loss and oxidation under adverse conditions. Moisture loss and weathering affect sample size and shape. Thermal expansion and contraction of the coal can similarly be an issue. Thus testing of the material requires close control of all aspects of the environmental conditions from the point of field sampling through to testing. Large block coal samples are excavated only from fresh exposures and are immediately wrapped to maintain moisture. They are then stored prior to use and after machining in a temperature and humidity controlled store at the temperature of 12°C to minimize moisture loss, loss of volatiles, and weathering prior to testing. During testing, specimens are either fully soaked in water or well wrapped in a plastic membrane. Whether the test specimen is soaked or wrapped, strain gauges cannot be glued to the specimen surface. Consequently, local strain gauges cannot be used for measuring local deformation and sensitive linear variable differential transformers (LVDTs) must be employed to measure external deformation and strain. In addition, since accurate LVDTs are also sensitive to temperature fluctuation, all tests were performed in a temperature controlled room with the temperature maintained at 21°C. Samples were allowed to thermally equilibrate prior to testing.

Direct Tensile Test

TEST EQUIPMENT

Practicality of the test method for routine geotechnical laboratory testing was an important consideration for development of the method. To satisfy this requirement, a standard direct shear box apparatus, available in most soil mechanics laboratories, was modified for the test. The direct shear box is

FIG. 1 Top view of modified direct shear box rig used for DTT.

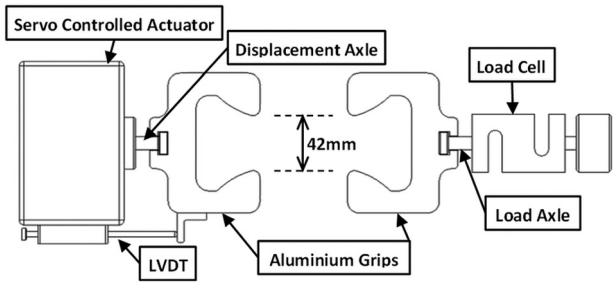

microprocessor controlled and can apply positive or negative shear loads along a predefined horizontal axis. Axial deformation is measured using an LVDT with accuracy of ±0.005 mm. A 5 kN S-Beam load cell with accuracy of 1 N measures the applied axial force. The loading or strain rate can be controlled via a computer attached to the system microprocessor. The shear box has been replaced by two aluminum grips that hold and axially pull the coal specimen. The sample is mounted on a low friction surface between the grips (see **Figs. 1** and **2(*a*)**). The shape of the grips was established to minimize tensile forces within the sample inside the grip and to produce smoothly varying stress and strain within the gripped region of the sample.

SAMPLE PREPARATION

Prior to the final selection of the most effective testing methodology, alternative specimen forms and test schemes were investigated. The three specimen forms were developed/tested sequentially in response to issues raised during the prior specimen testing. Images of the three specimen forms are shown in **Fig. 2**. The coal can be easily shaped while saturated if there are no defects or inclusions that are large relative to the scale of the final specimen form. Coal blocks were initially slabbed to 42 mm thick using a band saw and then the final shape was milled using a router. A template eases the final shape production. For the first design (shape I) the coal samples were cut into a bone shape with 42 by 42 mm rectangular cross section with an effective length of 84 mm (the length of the part with rectangular cross section) (see **Fig. 2(*a*)**). This design follows the common design used in unsaturated soil DTTs. For the second design (shape II), a rectangular column of coal was cut to a dimension of 42 by 42 by 70 mm (width by height by length). Hardwood ends that fit the grips were glued to the ends of the sample using an epoxy resin. A 5 N compression load was applied for 24 h to ensure that the samples were bonded and correctly aligned (**Fig. 2(*b*)**). The third sample design (shape III) corresponds to shape I, but is narrowed in the middle section of the sample. A 5 mm deep and 2 mm wide circumferential groove was cut into the sample at the sample mid-section (**Fig. 2(*c*)**). In this case, the specimen cross section at the groove

FIG. 2 The three specimen forms used for the DTT: (*a*) bone shape (shape I), (*b*) rectangular column glued to wood ends (shape II), (*c*) bone shape with groove around the middle section (shape III).

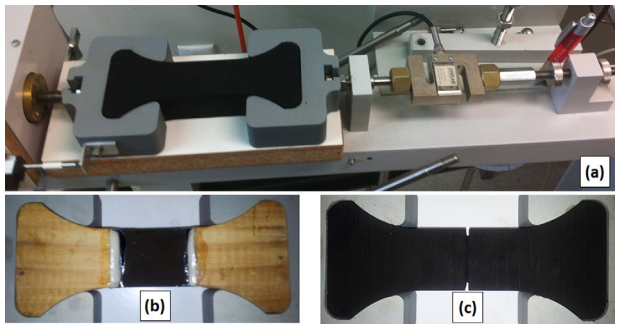

is decreased from 1764 to 1024 mm^2. This design ensures a predefined failure location in the sample.

DTT PROCEDURE AND RESULTS

Before starting each test, specimen position alignment was performed to ensure that the sample axis aligns with the axis formed by the centerline through the grips, the load cell axle, and the displacement axle. During alignment, a 1 N load was applied so that the specimen and grip were fully engaged. After alignment, the specimen and grips were wrapped in a plastic membrane to conserve specimen moisture content. Tensile displacement was then applied at a constant rate. As failure can be displacement rate dependent, two rates were adopted for the tests (0.002 and 0.05 mm/min). Load and displacement values were logged at appropriate time intervals.

Failure Mechanism of the Samples

Tests on shape I samples showed that, due to stress concentration developed at the interface of the grip and the coal, fractures initiated around the tip of the grips and rarely in the mid-section of the sample (see **Fig. 3(*a*)**). A few samples failed at the mid-section, but the location and cross sectional area of the fracture was too variable to be used in further calculations. Inspection of samples of shape II after each test showed that for most tests, failure cracks formed at or very close to the coal-wood interface in a random pattern (see **Fig. 3(*b*)**). This may have been due either to weaknesses in the epoxy bond or the epoxy affected the strength of the coal. The actual cause was not studied further. For samples of shape III, the failure was always in the middle section of the sample at the groove. While the groove concentrates stresses locally, observation of the fracture surfaces indicated that the edge effects were not likely to be over-biasing the apparent tensile strength. The model results described in the next section confirm this.

Load Deformation Relationship

The load-displacement curves for the tests on the samples of shape III are plotted in **Fig. 4**. The plots show that the coal

FIG. 3 Failure of typical samples of the three shapes: (*a*) Failure occurred in the coal next to the tip of the grip in shape I samples (as circulated in the picture), (*b*) Fracture initiated on coal-wood interface in specimen of shape II, and (*c*) failure occurred in the middle section of the sample at the groove.

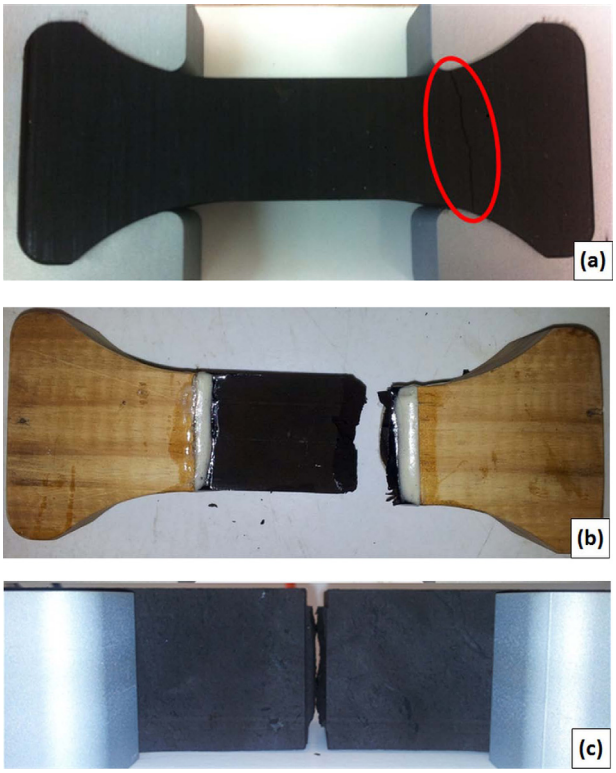

exhibits brittle behavior under tension. Before failure, it shows approximately linear elastic behavior. There is very little difference between the load deformation curves for different displacement rates. This suggests that the applied load rate has little effect on the tensile behavior of the material, even though the material is saturated and low permeability (on the order of 10^{-10} m/s). **Figure 4** shows that the peak tensile strength of the tested samples ranges from 95 to 125 kPa, with an average value of 101.4 kPa. The load–deformation curve fitting from FEM analysis, described later in this paper, shows the average stiffness of the samples is about 24 MPa.

FIG. 4 Results of direct tensile test on Australian brown coal.

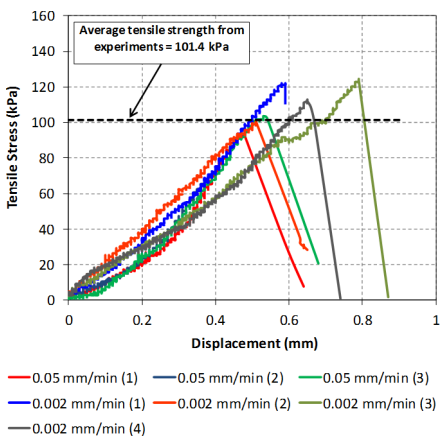

DTT NUMERICAL ANALYSIS

The impact of stress concentration around the failure plane caused by DTT on idealized bone shape samples can cause significant bias in laboratory results. To investigate the distribution of principal stresses for specimen shape III, numerical analysis has been performed using Abaqus/Explicit 6.12.1 (Dassault Systèmes 2012). The Brittle Cracking Model (BCM) in Abaqus/Explicit was employed to simulate the strain and brittle failure of the coal during a DTT. In this model, the Rankine criterion is used to detect crack initiation. This criterion states that a crack forms when the maximum principal tensile stress exceeds the tensile strength of the brittle material. The crack surface is taken to be normal to the direction of the maximum tensile principal stress (Dassault Systèmes 2012). In this model, cracking is irrecoverable and this makes the model suitable for modeling the DTT. The BCM follows linear elastic behavior before failure, so Poisson's ratio (ν) and Young's modulus (E) are required to calibrate the linear elastic behavior. In most brittle constitutive models, the post-failure behavior generally means giving the post-failure stress as a function of strain across the crack. However this approach introduces unreasonable mesh sensitivity into the results. It is generally accepted that a fracture energy based analysis is adequate for most practical purposes (Dassault Systèmes 2012). Hillerborg et al. (1976) defined the energy required to open a unit area of crack (G_f^I) as a material parameter, using brittle fracture concepts. With this approach the brittle behavior is characterized by a stress–displacement response rather than a stress–strain response. Having the crack normal displacement or length (u_n) and the maximum tensile strength (σ_t) post-failure stress-fracture energy can be calculated using Eq 1.

$$u_n = 2G_f^I/\sigma_t \tag{1}$$

When the failure criterion is satisfied and the displacement components at a material point reach the value defined as the failure displacement, the material point fails and all the stress components are set to zero and the element is removed from the mesh.

The model finite element geometry is shown in **Fig. 5**, where 6800 linear hexahedron elements (type C3D8R) form each bone-shape end and 53 000 quadratic tetrahedron elements (type C3D10M) are used to shape the middle part of the specimen. Since the stiffness of aluminum is much higher than stiffness of the coal, the two grips are modeled using analytical rigid surfaces to decrease the computational cost.

FIG. 5 Finite element geometry of specimen.

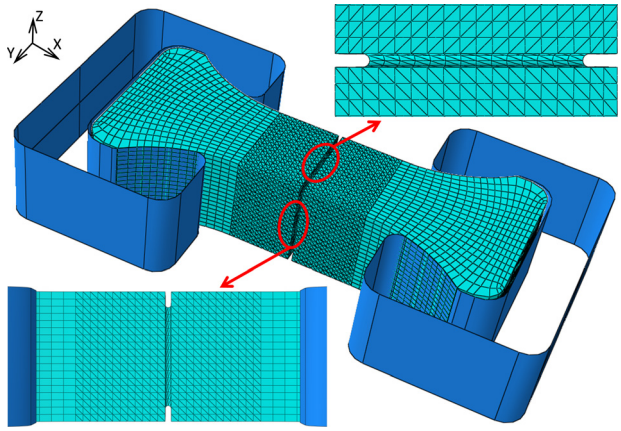

Considering **Figs. 2(*a*)** and **5**, three boundary conditions must be applied to the specimen: the specimen contact with the two grips and the vertical and shear resistance at the surface of the horizontal base plate of the test rig, which supports the specimen. The boundary conditions at the two ends are controlled using an appropriate formulation for coal-aluminum interface shear behavior. At the bottom of the sample the displacement and resistance vectors are specified to be Uz = URx = URy = 0.

Since the specimen may slide against the aluminum grips during the test, the coal–aluminum interface friction was taken into account. To measure the coal–aluminum interface friction, laboratory experiments were performed based on the technique suggested by Tolooiyan et al. (2009). In this technique, the friction strength between soil and other solid materials can be determined using a direct shear test. An aluminum plate of 60 by 60 mm was placed inside the lower compartment of a shear box. The upper box compartment was filled with coal (see **Fig. 6**). Several shear tests were performed at 3 different normal

FIG. 6 Measuring the shear strength between Australian brown coal and aluminum.

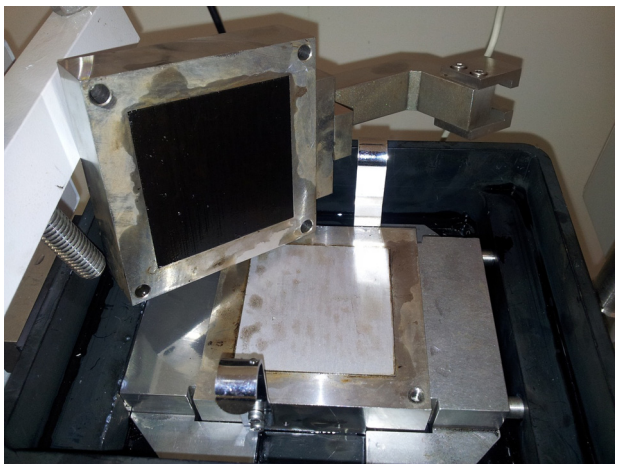

FIG. 7 Measured friction coefficient of ABC-aluminum interface.

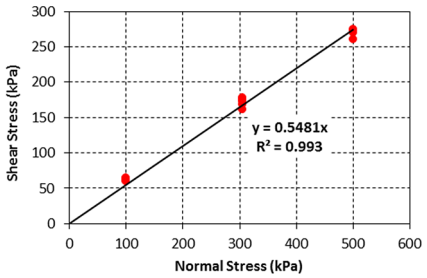

stress levels using this setup and a friction coefficient of $\mu = 0.55$ was measured (see **Fig. 7**).

Since Abaqus/Explicit was employed for the analysis and the aluminum grip was modeled using an analytical rigid body, the aluminum surface must be defined as a master surface and the specimen surface defined as the slave. This arrangement allows penetration of the stiff aluminum grip into the soft coal, subject to the constitutive behavior of the modeled specimen. The measured friction coefficient is then defined as the tangential friction coefficient using a kinematic contact/mechanical constraint formulation. This formulation adopts a predictor/corrector algorithm for model solution and therefore has no influence on the maximum stable time increment for the simulation analysis.

The brittle model was calibrated based on the laboratory observations. Poisson's ratio of the coal is assumed to be 0.1 for this analysis; however, it is believed that the Poisson's ratio has very little or no effect on the tensile behavior of materials. The test deformation curves were best fitted using the modeled tensile stiffness of 24 MPa. By adopting the average crack displacement of 0.1 mm measured form experiment on sample shape III and assuming a tensile strength value of 118 kPa, the apparent tensile strength calculated from FEM simulation of the performed experiment is 103 kPa (see **Fig. 8**). The 15 kPa difference between FEM input and output tensile strength values corresponds to the effect of stress concentration in the circumferential groove. Analysis of stress distribution shows that the principle stress around the edge of the failure plane is nearly 5 % higher than the developed axial stress. The developed stress around the failure plane is not distributed uniformly. This finding agrees with Coviello et al. (2005). The variation of 12 % between modeled and observed stress is acceptable for direct application of the results determined directly from the laboratory tests.

Brazilian Test

TEST EQUIPMENT AND SAMPLE PREPARATION

Adopting the same strategy employed for the direct tensile test, two loading plates made from aluminum were introduced at the

FIG. 8 Comparison between FEM and experiments.

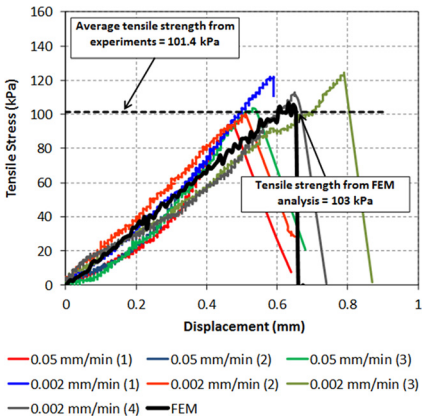

end of each grip with one connected to the load cell and other connected to the loading axle (see **Fig. 9**). In this setup, the sample can be loaded at a defined displacement rate until failure. Cylindrical coal specimens, 75.5 mm in diameter and 44 mm thick, were prepared by coring from a saturated block.

TEST PROCEDURES AND RESULTS

A displacement rate (determined from the FEM analysis described in the next section) of 0.002 mm/min was used to minimize excess pore water pressure at the center of the specimen. At this displacement rate, the test takes several hours. To conserve moisture during the test, the specimen was wrapped in a thin plastic membrane. Nine tests were performed with the displacement rate of 0.002 mm/min and the results are presented in **Fig. 10**. Using Eq 2 suggested by Mellor and Hawkes (1971), the average measured load value (F) gives a tensile strength of $S_t = 112$ kPa, when $D = 75.5$ mm and $t = 44$ mm.

$$S_t = \frac{2F}{\pi D t} \tag{2}$$

To study the effect of pore water pressure due to high speed loading, four tests were performed with a displacement rate of 0.1 mm/min. As shown in **Fig. 11**, the average tensile strength

FIG. 9 Plan view of modified direct shear box rig to be used for BT.

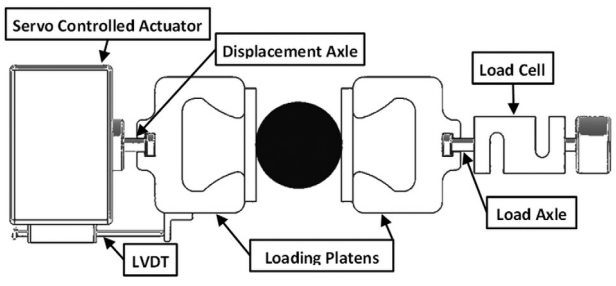

FIG. 10 Test and modeled results of Brazilian test on Australian brown coal (displacement rate 0.002 mm/min).

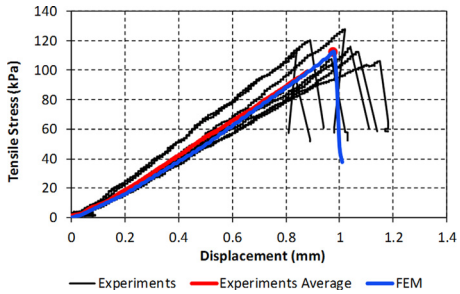

measured from these tests is about 90 kPa, 20 % less than the tensile strength value measured from BT at the loading rate of 0.002 mm/min. This effect is considered in the next section in the numerical analysis.

BT NUMERICAL ANALYSIS

The finite element analysis using Abaqus followed the same modeling strategy and used the same model form, constitutive relationships and input parameters employed for the direct tensile test analysis. The Brazilian test specimen was modeled with 44 900 linear hexahedron elements (type C3D8R). The aluminum plates were modeled using analytical rigid surfaces (**Fig. 12**).

As for the BT simulation, three boundary conditions were applied: two for the aluminum plates and the third for the horizontal plate, which supports the specimen that account for aluminum coal friction and surface displacement of the coal at the contact surfaces.

During the analysis, one of the plates is fully fixed and the other one moves slowly in the x-direction to compress the sample. The load produced is then measured from a reference point on the fixed plate and applied displacement is measured from a reference point on the moving plate.

The constitutive model input parameters were applied based on the laboratory experiment and FEM analysis of DTT.

FIG. 11 Tensile stress versus displacement for displacement rate of 0.1 mm/min.

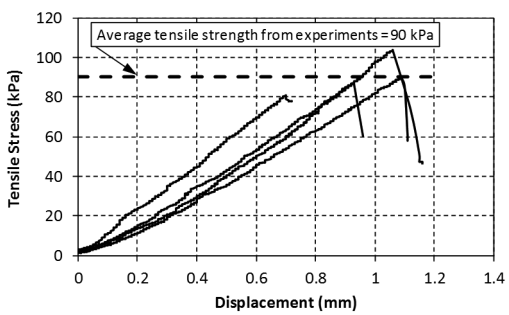

FIG. 12 FEM model of BT.

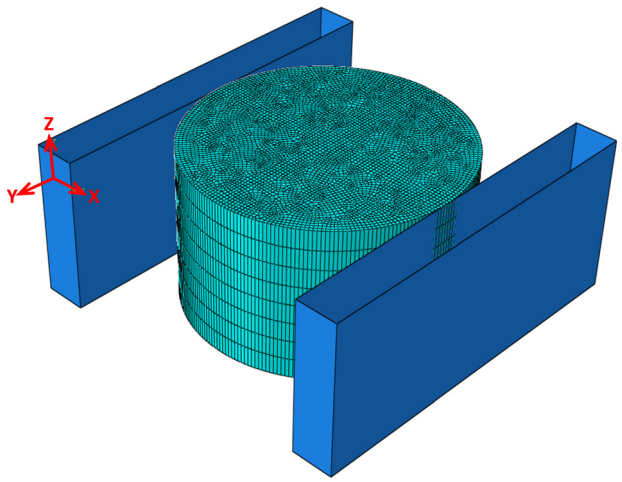

Based on the DTT results, 118 kPa was assumed as the coal tensile strength. The values of Poisson's ratio (ν), crack opening length (u_n), and fracture energy (G_f^I) used were 0.1, 0.1 mm and 0.006 N/mm, respectively. The only model parameter to be re-calibrated was the coal stiffness (E). Since the calibrated stiffness of 24 MPa from the DTT is based on extension and not compression, this value should be re-calibrated for a compression test. Considering bi-modularity of organic rocks, the stiffness in compression is assumed be 2 to 3 times more than the stiffness in tension. Hence, the compressive stiffness was assumed to be 2.5 times more than the tensile stiffness (i.e., 60 MPa). This stiffness value was double-checked after FEM analysis and slope of load-displacement curve has been compared with the one from laboratory measurements (see **Fig. 10**).

Displacement of the BT specimen before and after failure is shown in **Fig. 13**. **Figure 14** shows the simulated load–displacement curve. The stress–displacement curve is also reproduced earlier in **Fig. 10** as a comparison with the laboratory test results. Load–displacement profile in **Fig. 14** indicates a sudden failure of the specimen when the load reaches 585 N. Using Eq 2, this load value can be translated to tensile strength of 112 kPa.

The calculated tensile strength from this simulation (112 kPa) is 5.1 % less than the input tensile strength (118 kPa). This underestimation agrees with the results of Yu et al. (2006) and Fahimifar and Malekpour (2012). They used FEM to analyze stress distribution in a BT specimen and confirmed that, since tensile stress is not uniformly distributed throughout the failure plan, the BT may marginally underestimate a material's tensile strength. They suggest a correction factor, which takes the dimension of sample into account, should be applied for more accurate measurement. Yu et al. (2006) suggested Eq 3 for correcting the result of a BT for rock:

$$S_{tc} = (\mathrm{jk} + 1)\frac{2F}{\pi Dt} \tag{3}$$

FIG. 13

Displacement profile (in mm): (*a*) before test, (*b*) at failure onset, and (*c*) just after failure.

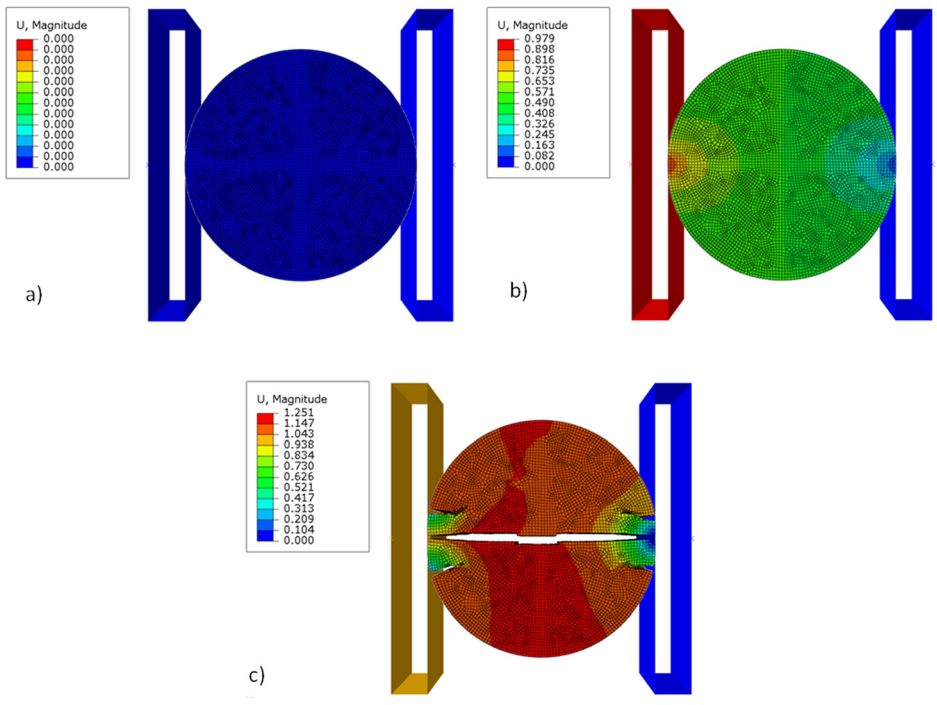

FIG. 14 Load and stress profile from FEM analysis of BT.

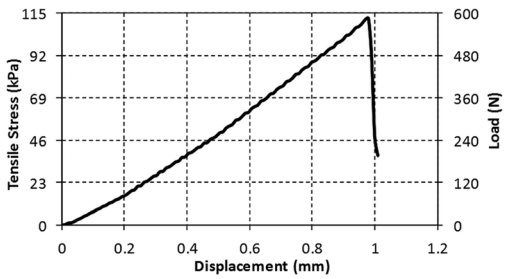

where:

S_{tc} = corrected tensile strength,

j = an empirical factor related to the general character of rock that is smaller than one (e.g., 0.26 for medium hard rock), and

k = the ratio of specimen thickness and diameter.

Using Eq 3, the measured tensile strength from FEM analysis (112 kPa) can be corrected and equalized with the input tensile strength (118 kPa) using $j = 0.09$.

To illustrate the difference between principal stress and developed stress perpendicular to the failure plane, stress magnitude and orientation at failure onset are shown in **Figs. 15** and **16**, respectively. From these figures, it is clear that the principal stress is developed uniformly on the failure plane.

FIG. 15 Stress distribution at onset of failure: (*a*) principal stress, (*b*) stress perpendicular to the failure plane.

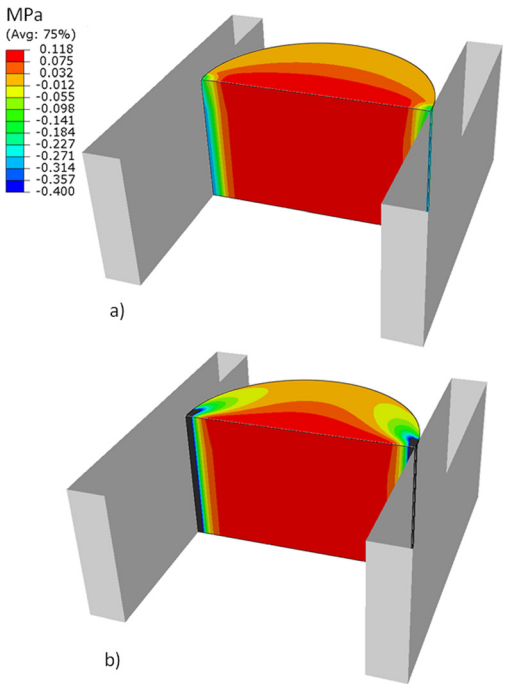

FIG. 16 Stress direction at onset of failure: (*a*) principal stress, (*b*) stress perpendicular to the failure plane.

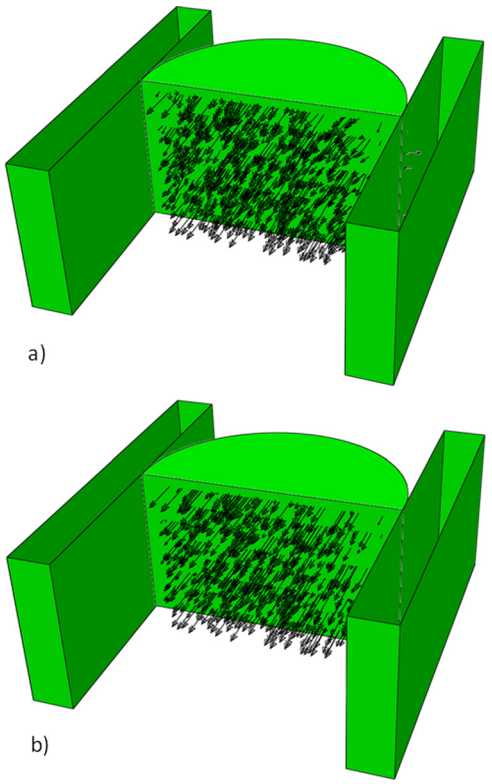

Excess pore water pressure caused by applied deformation can be a concern. Unfortunately, simulation of the pore water pressure distribution can only be performed with Abaqus/Standard, while the crack propagation analysis must be performed with Abaqus/Explicit. These two analyses cannot be combined together with the current setup of Abaqus 6.12. To analyze the effect of pore water pressure, two tests were simulated using Abaqus/Standard, one with an applied displacement rate of 0.002 mm/min (Test A) and the other at 0.1 mm/min (Test B). The coal permeability and void ratio values were 4×10^{-7} mm/s and 1.5, respectively. Since crack propagation and failure cannot be modeled in this analysis, the developed effective stress and excess pore water pressure on the failure plane are investigated when effective stress reaches 118 kPa at the center of specimen. As shown in **Figs. 17(*a*)** and **17(*b*)**, the pattern of principal effective stresses when the midpoint value reaches 118 kPa is similar for both tests. However, for Test A, axial displacement is 0.9 mm (**Fig. 17(*c*)**), but for Test B, axial displacement is 0.77 mm at the time that 118 kPa principal stress is reached (**Fig. 17(*d*)**). From **Fig. 17(*e*)** and **17(*f*)**, it is clear that in Test B pore water pressure at center of specimen is as high as 30 kPa, which is the cause of the earlier failure in the specimen. The difference between the principle stress and the pore water pressure is in the range of 90 kPa, which is very close to the tested tensile strength shown in **Fig. 11**.

FIG. 17 Developed effective stress and pore water pressure in Test A and B.

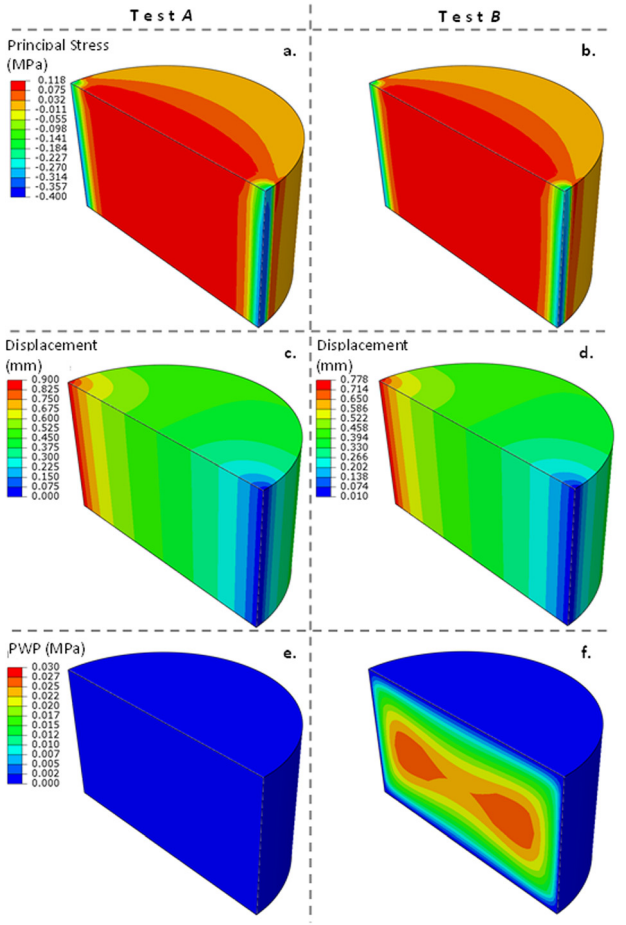

Summary and Concluding Remarks

A direct shear box testing rig has been modified to measure the tensile strength of Australian brown coal as an organic intermediate geotechnical material. Two modifications were undertaken: the first to develop a procedure for direct tensile testing and the second to carry out Brazilian tests. Alternative specimen shapes were examined for the direct tensile test. The most appropriate was found to be a bone shaped sample with a 2 mm wide groove, 5 mm deep machined around the mid-section of the sample. Loading rate for the direct tensile test was not found to be important, while loading rate for the Brazilian test was a significant determinant of the apparent tensile strength of the coal. The rate dependency was assessed to be due to the development of increased pore pressures in the sample at high loading rates. Results from the two test methods were found to be comparable with the average coal tensile strength from the direct tensile test being 101.4 kPa, while the average for the Brazilian test was observed to be 112 kPa.

To investigate the effect of stress concentration in both tests, a constitutive brittle crack model was calibrated and employed for finite element analysis using Abaqus/Explicit code. Numerical results showed that the actual tensile strength of tested material can be slightly higher (10 %–12 %) than the direct test value and 5 % higher than the Brazilian Test value. An actual average coal tensile strength of 118 kPa is derived from the model calculation. The pore pressure distribution for the Brazilian test was also modeled using Abaqus/Standard. Although pore pressure and tensile failure cannot be modeled simultaneously the pore pressure modeling illustrates the sensitivity of the peak stress in the Brazilian test to the excess pore pressure distribution in the specimen. While the placement of the groove around the mid-section of the direct tensile test specimen does impact the observed tensile strength, this technique does show considerable benefits in terms of the reliability and repeatability of the test method.

The testing carried out has demonstrated the utility of both methods for tensile strength measurement for brown coal. The methods should be similarly applicable to other soft brittle rocks. It has also demonstrated the tendency for both tests to marginally underestimate the actual tensile strength, but the errors are within the uncertainty bounds arising from the natural variability of brown coal. This observation accords with previous work with other materials.

The potential for applying a correction factor for both tests to improve the accuracy of the methods for Brown coal does exist, but further work would be required to confirm the form of the correction, including the value of any empirical constants related to the stiffness of the material and geometry of the test specimen. The empirical equation proposed by Yu et al. (2006) could prove to be a useful starting point for such an investigation.

ACKNOWLEDGMENTS

Financial support for this research has been provided by Earth Resources Regulation of the Victorian State Government Department of State Development, Business and Innovation. The authors would like to thank Mr. Wayne Powrie, who prepared the equipment and specimens for this research. The assistance of AGL Loy Yang and GHD Australia is also acknowledged for their support and help with sample collection.

References

Ajaz, A. and Parry, R., 1974, "An Unconfined Direct Tension Test for Compacted Clay," *ASTM J. Test. Eval.*, Vol. 2, No. 3, pp. 163–172.

Amarasiri, A. L., Costa, S. and Kodikara, J. K., 2011, "Determination of Cohesive Properties for Mode I Fracture From Compacted Clay Beams," *Can. Geotech. J.*, Vol. 48, No. 8, pp. 1163–1173.

ASTM D3967-08, 2008: Standard Test Method for Splitting Tensile Strength of Intact Rock Core Specimens, *Annual Book of ASTM Standards*, ASTM International, West Conshohocken, PA.

Australia Mineral Resource, 2011, The Australian Atlas of Mineral Resources, Mines, and Processing Centres, Commonwealth of Australia.

Barla, G. and Innaurato, N., "Indirect Tensile Testing of Anisotropic Rocks," *Rock Mech.*, Vol. 5, No. 4, 1973, pp. 215–230.

Butenuth, C., De Freitas, M. H., Al–Samahiji, D., Park, H. D., Cosgrove, J. W. and Schetelig, K., 1993, "Observations on the Measurement of Tensile Strength Using the Hoop Test," *Int. J. Rock Mech. Min. Sci. Geomech. Abs.*, Vol. 30, No. 2, pp. 157–162.

Cai, M. and Kaiser, P. K., "Numerical Simulation of the Brazilian Test and the Tensile Strength of Anisotropic Rocks and Rocks with Pre–Existing Cracks," *Int. J. Rock Mech. Min. Sci.*, Vol. 41, No. 3, 2004, pp. 478–483.

Colback, P. S. B., 1966, "An Analysis of Brittle Fracture Initiation and Propagation in the Brazilian Test," *Proceedings of the First Congress of the International Society for Rock Mechanics. International Society for Rock Mechanics*, Lisbon, Portugal, July 9–13, pp. 385–391.

Coviello, A., Lagioia, R. and Nova, R., "On the Measurement of the Tensile Strength of Soft Rocks.," *Rock Mech. Rock Eng.*, Vol. 38, No. 4, 2005, pp. 251–273.

Dassault Systèmes, 2012, *Abaqus*, 6.12 ed., Dassault Systèmes, Dassault Systèmes Simulia Corp., Providence, RI.

DPI, 2012, *About Victoria's Brown Coal*, Department of Environment and Primary Industries, Melbourne, Australia.

Exadaktylos, G. E. and Kaklis, K. N., 2001, "Applications of an Explicit Solution for the Transversely Isotropic Circular Disc Compressed Diametrically," *Int. J. Rock Mech. Min. Sci.*, Vol. 38, No. 2, pp. 227–243.

Fahimifar, A. and Malekpour, M., 2012, "Experimental and Numerical Analysis of Indirect and Direct Tensile Strength Using Fracture Mechanics Concepts," *Bull. Eng. Geol. Environ.*, Vol. 71, No. 2, pp. 269–283.

GBStandards-T50266, 1999: Standard for Tests Method of Engineering Rock Masses, The National Standards Compilation Group of People's Republic of China, Beijing, China, p. 20.

Haberfield, C. M., 1997, "Pressuremeter Testing in Weak Rock and Cemented Sand," *Proc. ICE–Geotech. Eng.*, Vol. 125, No. 3, pp. 168–178.

Hudson, J. A., 1969, "Tensile Strength and the Ring Test," *Int. J. Rock Mech. Min. Sci. Geomech. Abs.*, Vol. 6, No. 1, pp. 91–97.

Hudson, J. A., Brown, E. T. and Rummel, F., "The Controlled Failure of Rock Discs and Rings Loaded in Diametral Compression," *Int. J. Rock Mech. Min. Sci. Geomech. Abs.*, Vol. 9, No. 2, 1972, pp. 241–248.

ISRM, 1977, Suggested Methods for Determining Tensile Strength of Rock Materials, The Society, Lisborn, Portugal.

Jaeger, J. C., 1967, "Failure of Rocks Under Tensile Conditions," *Int. J. Rock Mech. Min. Sci. Geomech. Abs.*, Vol. 4, No. 2, pp. 219–227.

Jaeger, J. C. and Hoskins, E. R., 1966, "Rock Failure Under the Confined Brazilian Test," *J. Geophys. Res.*, Vol. 71, No. 10, pp. 2651–2659.

Li, D. and Wong, L., 2013, "The Brazilian Disc Test for Rock Mechanics Applications: Review and New Insights," *Rock Mech. Rock Eng.*, Vol. 46, No. 2, pp. 269–287.

Lu, N., Wu, B. and Tan, C., 2007, "Tensile Strength Characteristics of Unsaturated Sands," *ASCE J. Geotech. Geoenviron. Eng.*, Vol. 133, No. 2, pp. 144–154.

Mellor, M. and Hawkes, I., 1971, "Measurement of Tensile Strength by Diametral Compression of Discs and Annuli," *Eng. Geol.*, Vol. 5, No. 3, pp. 173–225.

Tolooiyan, A., Abustan, I., Selamat, M. R. and Ghaffari, S., 2009, "A Comprehensive Method for Analyzing the Effect of Geotextile Layers on Embankment Stability," *Geotext. Geomembr.*, Vol. 27, No. 5, 399–405.

Vesga, L. and Vallejo, L., 2006, "Direct and Indirect Tensile Tests for Measuring the Equivalent Effective Stress in a Kaolinite Clay," *Fourth International Conference on Unsaturated Soils*, Carefree, Arizona, April 2–6, ASCE, Reston, VA, pp. 1290–1301.

Xue, J. and Tolooiyan, A., 2012, "Reliability Analysis of Block Sliding in Large Brown Coal Open Cuts," *The 2012 World Congress on Advances in Civil, Environmental, and Materials Research*, Techno–Press Journals, Korea, pp. 1578–1587.

Yu, Y., Yin, J. and Zhong, Z., 2006, "Shape Effects in the Brazilian Tensile Strength Test and a 3D FEM Correction," *Int. J. Rock Mech. Min. Sci.*, Vol. 43, No. 4, 623–627.